

Comsol Conference 2008

Nonlinear Ferrohydrodynamics of Magnetic Fluids

Markus Zahn
Massachusetts Institute of Technology
Department of Electrical Engineering and Computer Science
Laboratory for Electromagnetic and Electronic Systems

OUTLINE

1. Introduction to Ferrohydrodynamics
2. Applications to Magnetic Resonance Imaging (MRI)
3. Applications to Increasing Power Transformer Electric Breakdown Strength
4. Ferrohydrodynamic Instabilities
5. Dielectric Analog: Von Quincke Electrorotation

1. INTRODUCTION TO FERRODYNAMICS

FERROHYDRODYNAMICS

$$\bar{F} = \begin{cases} \bar{J} \times \bar{B} - \frac{1}{2} H^2 \nabla \mu & \text{(Linear Magnetization)} \\ \bar{J} \times \mu_o \bar{H} + \mu_o (\bar{M} \bullet \nabla) \bar{H} & \text{(Magnetizable Medium)} \end{cases} \quad \text{(Force Density)}$$

$$\tau = \sigma \mu \ell^2 \quad \text{(Magnetic Diffusion Time)}$$

$$\delta = \sqrt{\frac{2}{\omega \mu \sigma}} \quad \text{(Skin Depth)}$$

$$R_m = \frac{\sigma \mu \ell^2}{\ell / v} = \sigma \mu v \ell \quad \text{(Magnetic Reynolds Number)}$$

ELECTROHYDRODYNAMICS

$$\bar{F} = \begin{cases} \rho_f \bar{E} - \frac{1}{2} E^2 \nabla \epsilon & \text{(Linear Dielectric)} \\ \rho_f \bar{E} + (\bar{P} \bullet \nabla) \bar{E} & \text{(Polarizable Dielectric)} \end{cases} \quad \text{(Force Density)}$$

$$\tau = \epsilon / \sigma \quad \text{(Dielectric Relaxation Time)}$$

$$R_e = \frac{\epsilon / \sigma}{\ell / v} = \frac{\epsilon v}{\sigma \ell} \quad \text{(Electric Reynolds Number)}$$

Ferrofluids

Colloidal dispersion of permanently magnetized particles undergoing rotational and translational Brownian motion.

Established applications

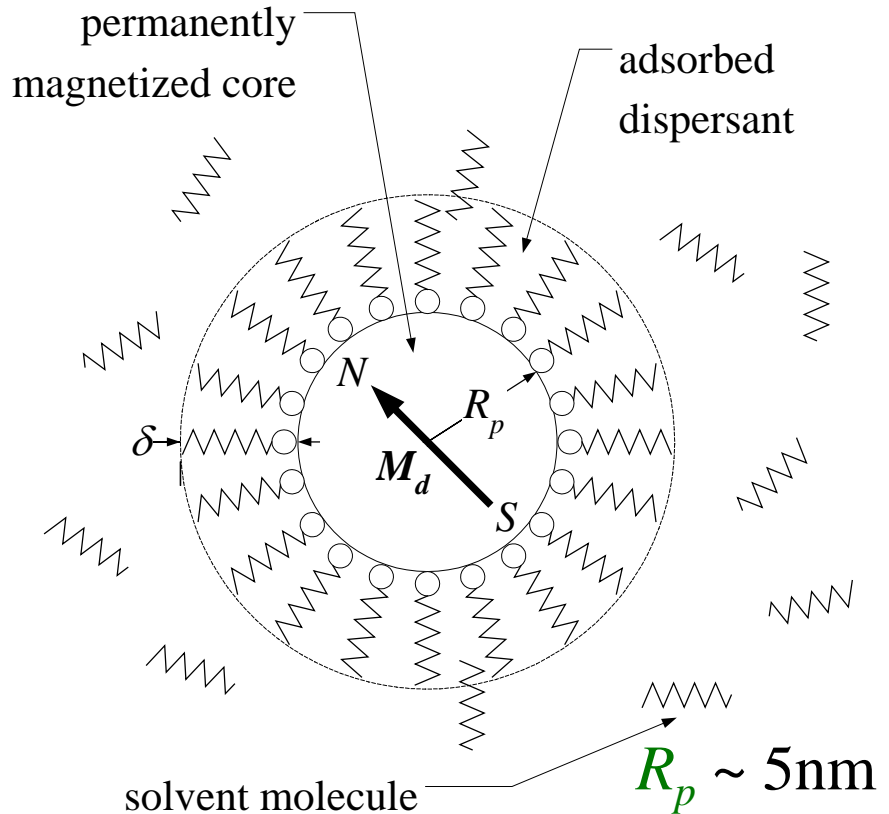
rotary and exclusion seals, stepper motor dampers, heat transfer fluids

Emerging applications

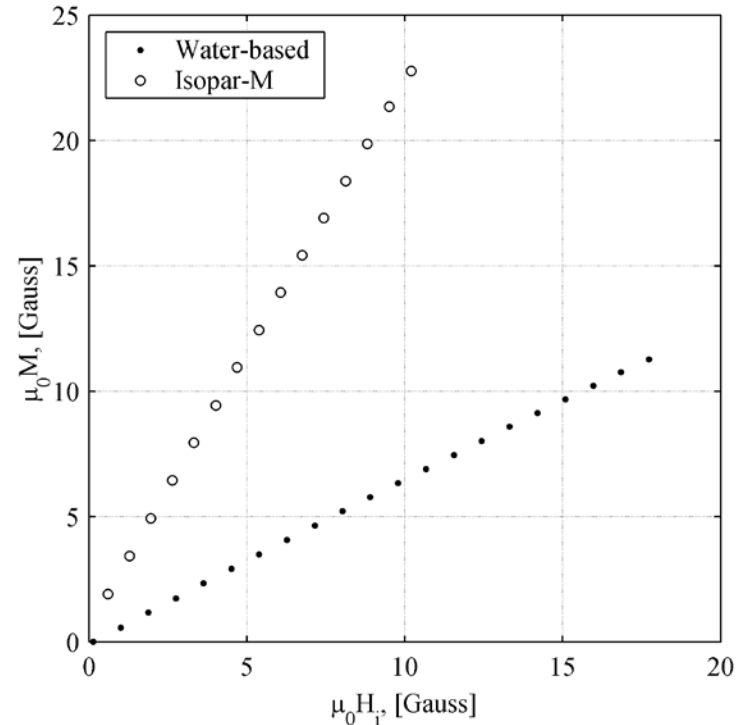
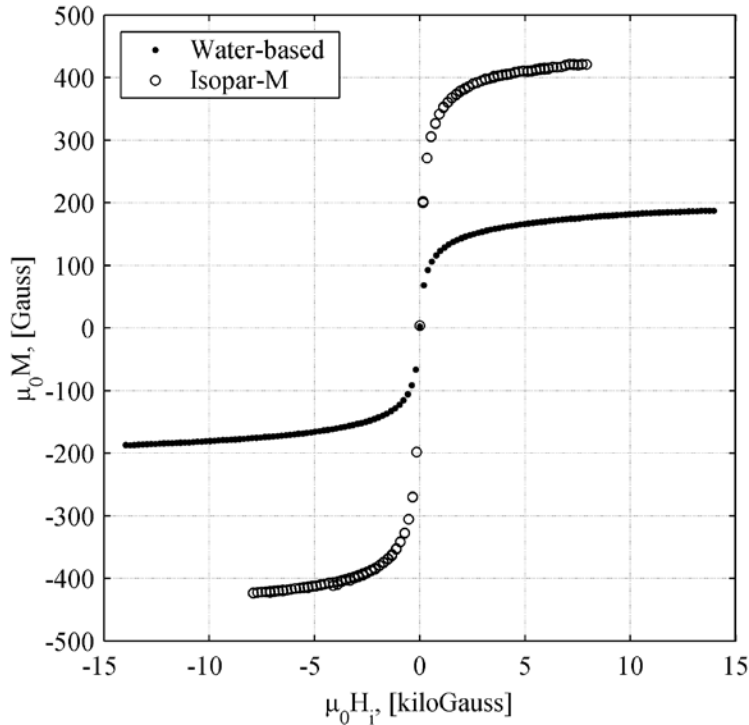
MEMS/NEMS – motors, generators, actuators, pumps

Bio/Medical – cell sorters, biosensors, magnetocytolysis, targeted drug delivery vectors, *in vivo* imaging, hyperthermia, immunoassays

Separations – magneto-responsive colloidal extractants



Ferrofluid Magnetic Properties



Water-based Ferrofluid

$$\mu_0 M_s = 203 \text{ Gauss}$$

$$\phi = 0.036 ; \chi_0 = 0.65, \rho = 1.22 \text{ g/cc}, \eta \approx 7 \text{ cp}$$

$$d_{\min} \approx 5.5 \text{ nm}, d_{\max} \approx 11.9 \text{ nm}$$

$$\tau_B = 2-10 \mu\text{s}, \tau_N = 5 \text{ ns}-20 \text{ ms}$$

Isopar-M Ferrofluid

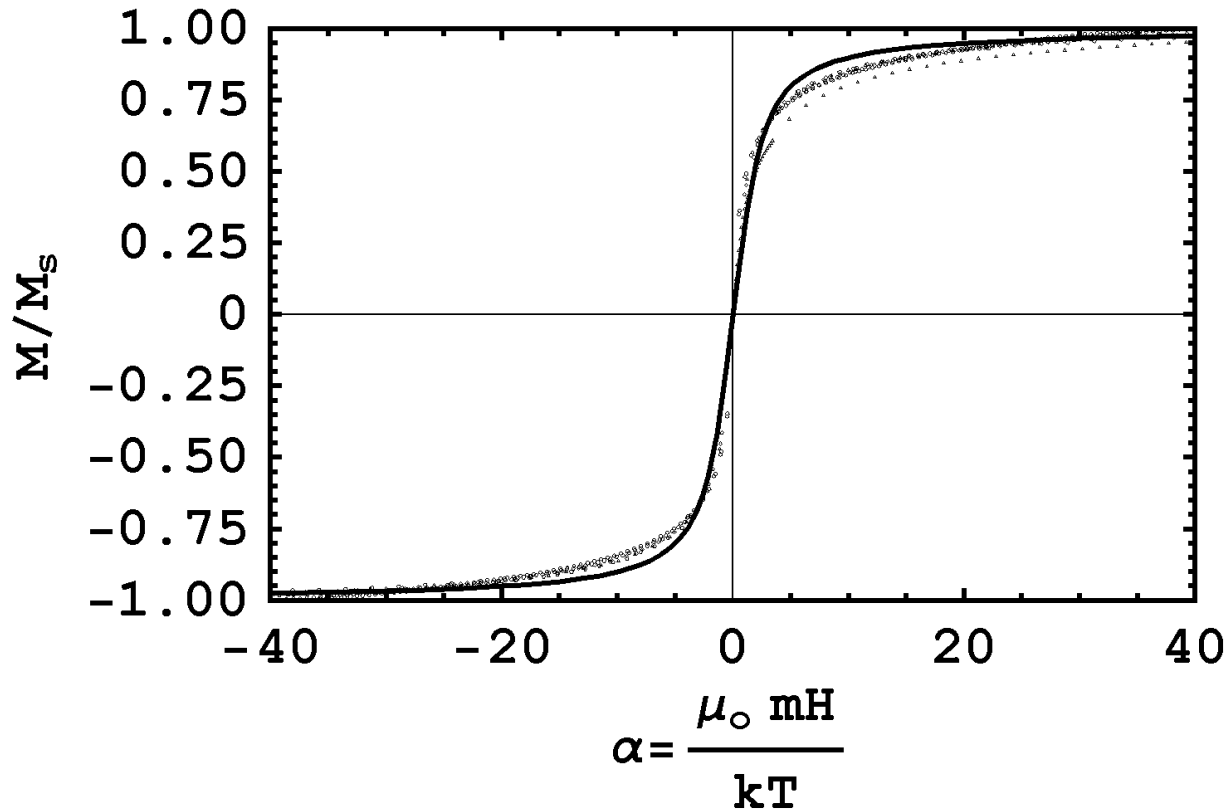
$$\mu_0 M_s = 444 \text{ Gauss}$$

$$\phi = 0.079 ; \chi_0 = 2.18, \rho = 1.18 \text{ g/cc}, \eta \approx 11 \text{ cp}$$

$$d_{\min} \approx 7.7 \text{ nm}, d_{\max} \approx 13.8 \text{ nm}$$

$$\tau_B = 7-20 \mu\text{s}, \tau_N = 100 \text{ ns}-200 \text{ s}$$

Langevin Equation $[\frac{M}{M_s} = \coth\alpha - \frac{1}{\alpha}]$



Measured magnetization (dots) for four ferrofluids containing magnetite particles ($M_d = 4.46 \times 10^5$ Ampere/meter or equivalently $\mu_0 M_d = 0.56$ Tesla) plotted with the theoretical Langevin curve (solid line). The data consist of Ferrotec Corporation ferrofluids: NF 1634 Isopar M at 25.4° C, 50.2° C, and 100.4° C all with fitted particle size of 11 nm; MSG W11 water-based at 26.3° C and 50.2° C with fitted particle size of 8 nm; NBF 1677 fluorocarbon-based at 50.2° C with fitted particle size of 13 nm; and EFH1 (positive α only) at 27° C with fitted particle size of 11 nm. All data falls on or near the universal Langevin curve indicating superparamagnetic behavior.

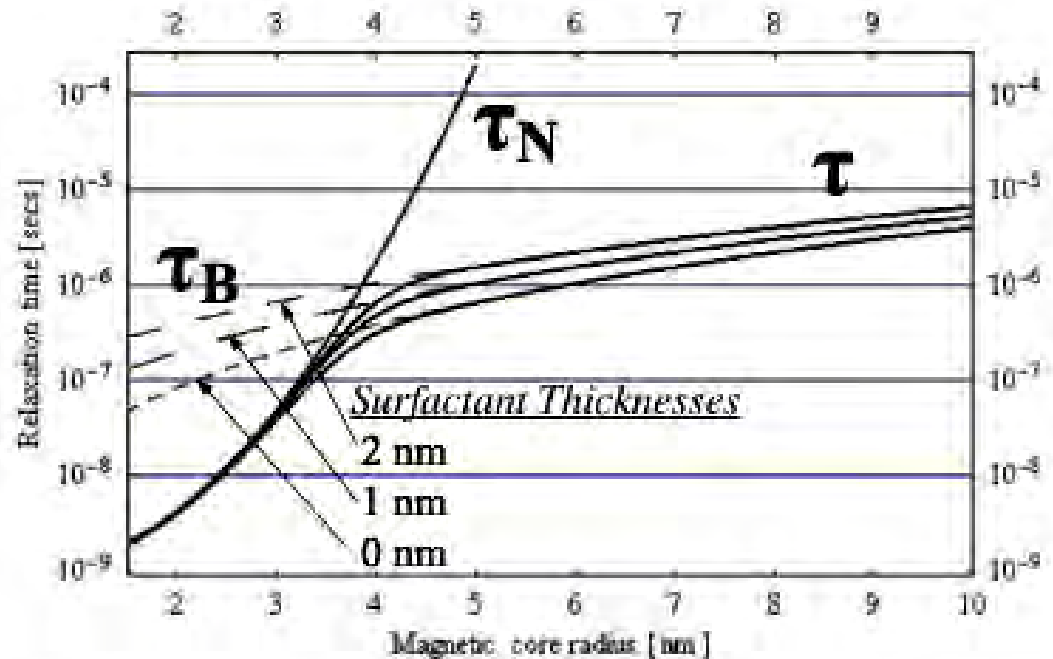
Characteristic Brownian and Néel Relaxation Times

$$\tau_B = 3V_h \frac{\eta_0}{kT}$$

$$\tau_N = \frac{1}{f_0} \exp\left(\frac{K_a V_c}{kT}\right)$$

$$\frac{1}{\tau} = \frac{1}{\tau_B} + \frac{1}{\tau_N}$$

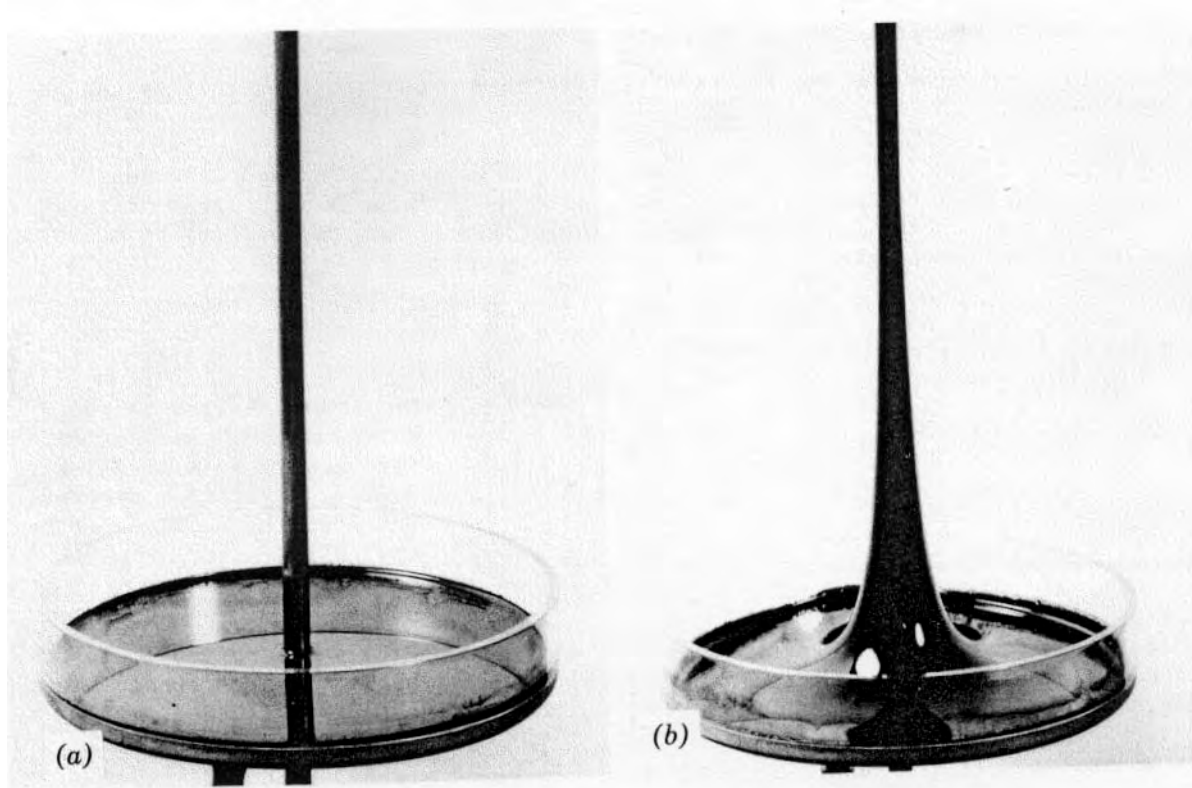
Effect of Radius Size on Ferrofluid Time Constant



The ferrofluid time constant, τ , is due to either the Néel (τ_N) or Brownian (τ_B) relaxation times, depending on the particle's radius.

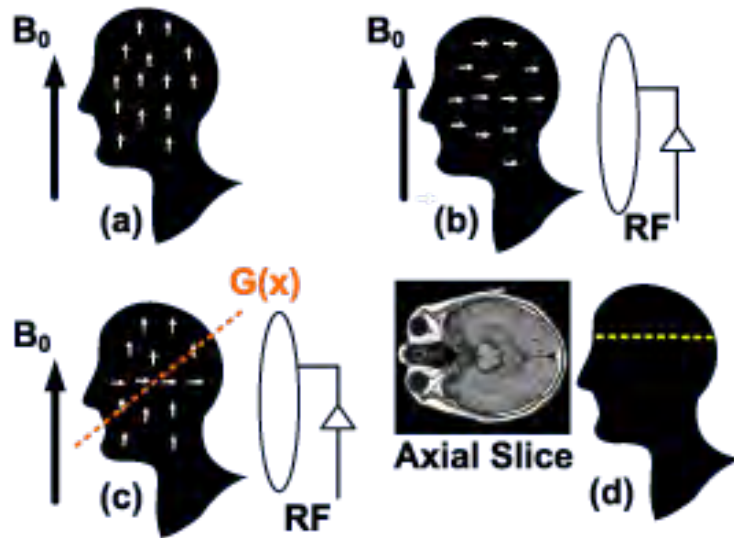
$$\tau \square 10^{-6} \text{ s} \quad (7\text{-}8 \text{ nm water-based magnetite})$$

Ferrofluid Magnetization Force



A magnetizable liquid is drawn upward around a current-carrying wire.

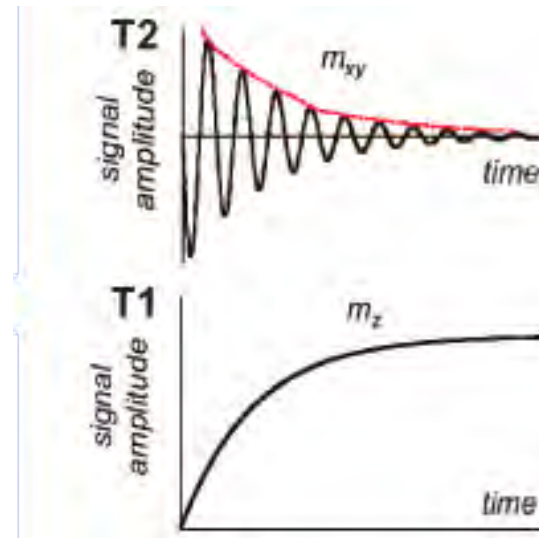
2. Application of Magnetic Media to Magnetic Resonance Imaging (MRI)



The fundamental elements of MRI are (a) dipole alignment, (b) RF excitation at Larmor frequency $f = \gamma B_0 / 2\pi$, (c) slice selection and (d) image reconstruction.

Larmor Frequency $f = \gamma B_0 / 2\pi = 42.576 \text{ MHz/Tesla}$ for Protons

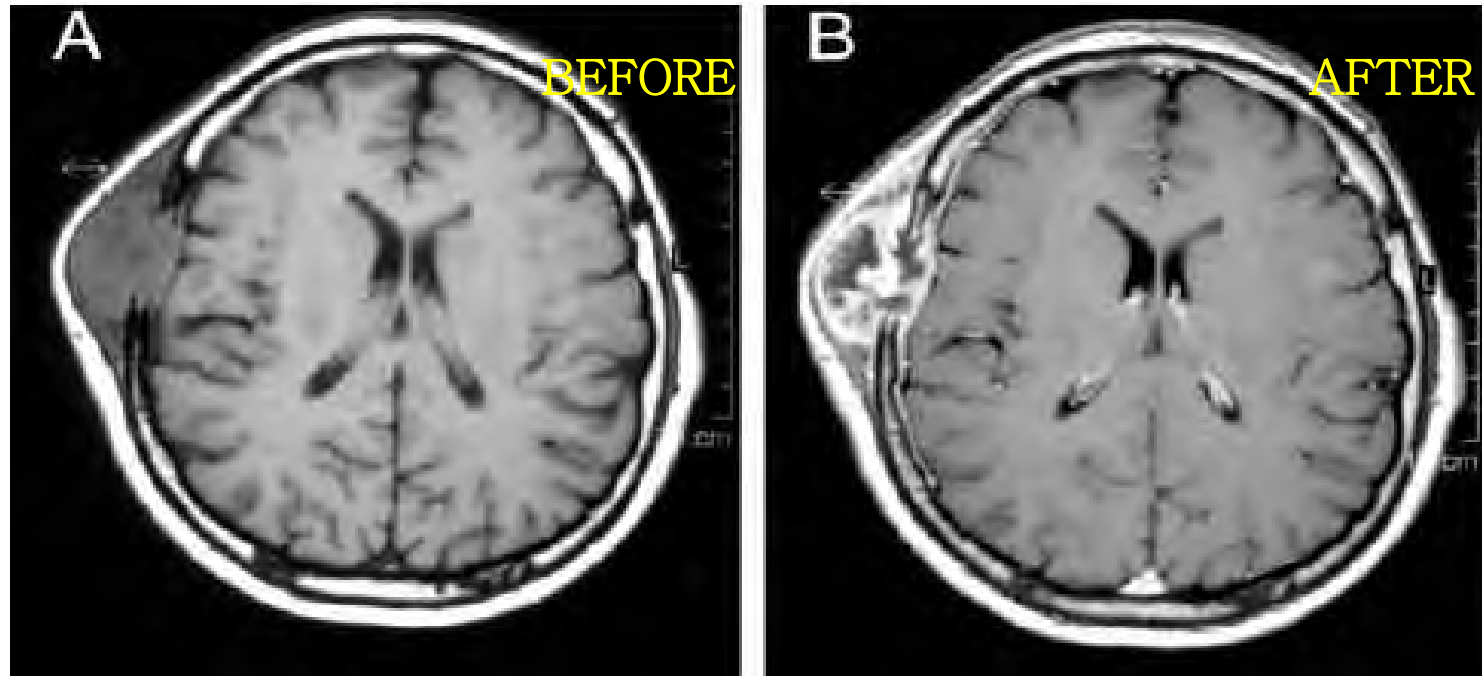
(γ = gyromagnetic ratio, $\frac{\gamma}{2\pi} = 42.576 \text{ MHz/Tesla}$ for ^1H nucleus.)



T2 decay is characterized by the exponential decay envelope of the magnetization signal in the $\{xy\}$ plane after excitation. T1 recovery is characterized by the exponential growth of the magnetization along the z axis as the vector returns to the equilibrium magnetization.

Ferrofluids as Contrast Agents in MRI

MRI Image of the Brain (A) Before and (B) After Gadolinium contrast enhancement

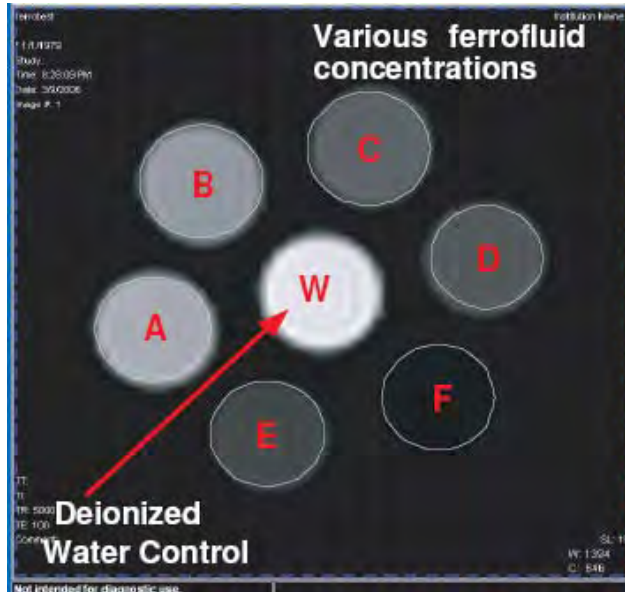


Two categories of contrast agents in MRI:

- Ferrofluids called superparamagnetic iron oxide (SPIO) contrast agents (currently smaller market share)
- Gadolinium-based contrast agents

T1 weighted MRI of the brain (a) before and (b) after Gadolinium contrast enhancement, showing a metastatic deposit involving the right frontal bone with a large extracranial soft tissue component and meningeal invasion. This figure comes from a case report of suspected dormant micrometastasis in a cancer patient.

Effect of Ferrofluid on Image Contrast



Vial	Solid Volume Fraction, ϕ	T1 in ms	T2 in ms
A	4.7×10^{-7}	1706	265
B	1.15×10^{-6}	1345	108
C	2.2×10^{-6}	1009	74
D	2.75×10^{-6}	887	57
E	5.5×10^{-6}	-	27
F	1.4×10^{-5}	-	20

T1 and T2 results for various water based ferrofluid solid volume fractions, ϕ . At very high concentrations ($\phi > 5 \times 10^{-6}$), the SNR was not sufficient to allow for the accurate determination of T1 relaxation times.

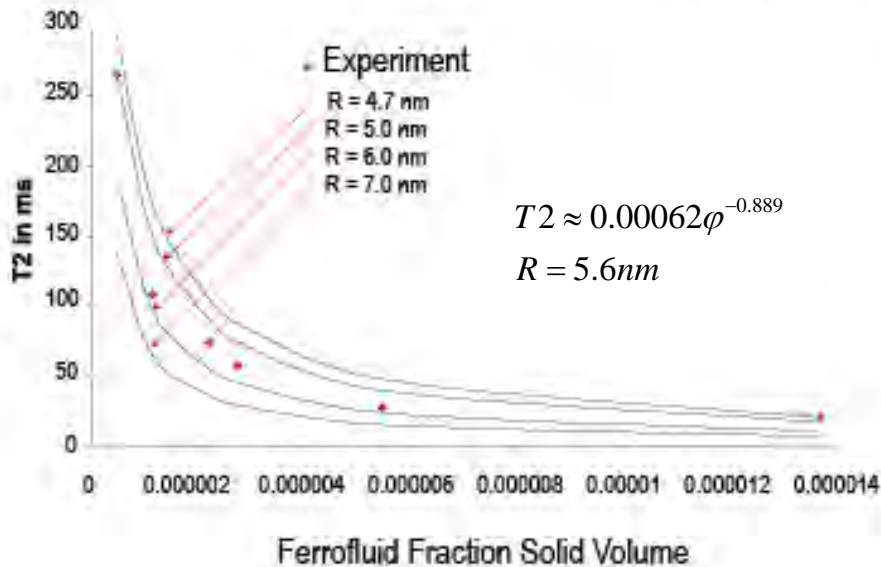
A : $\phi = 4.7 \times 10^{-7}$ ϕ =Percentage
 F : $\phi = 1.4 \times 10^{-5}$ solid volume

Experiments at the Martinos Center for
 Biomedical Imaging (MGH)

Pádraig Cantillon-Murphy, “On the Dynamics of Magnetic Fluids in Magnetic Resonance Imaging”, Massachusetts Institute of Technology PhD thesis, May 2008.

T2 Time Constant as Function of Ferrofluid Solid Volume Fraction ϕ

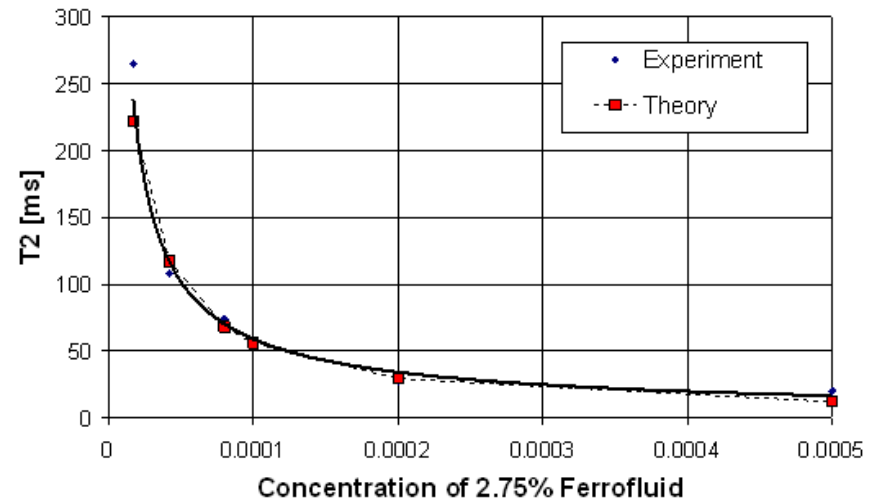
T2 Experimental and Theoretical Results



Comparison of the theoretical prediction for T2 at various superparamagnetic particle radii with the experimental results over a range of MSG W11 water-based ferrofluid concentrations of the original 2.75% solution by volume.

Ferrofluid Contribution to MRI Relaxation Time, T2

T2 Dependence on Ferrofluid Concentration

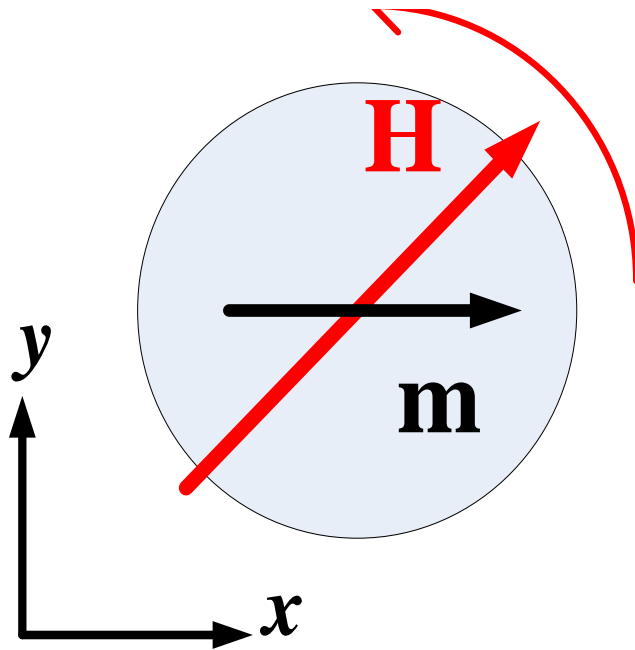


Particle size fit: $R \approx 5.6 \text{ nm}$

Pádraig Cantillon-Murphy, “On the Dynamics of Magnetic Fluids in Magnetic Resonance Imaging”, Massachusetts Institute of Technology PhD thesis, May 2008.

Conservation of Linear and Angular Momentum

$$0 = \rho \mathbf{g} + \mu_0 \mathbf{M} \cdot \nabla \mathbf{H} - \nabla p + (\eta + \zeta) \nabla^2 \mathbf{v} + 2\zeta (\nabla \times \boldsymbol{\omega})$$



$$\mathbf{M} = N\mathbf{m}$$

N = num. particles per m^3

ζ = vortex viscosity

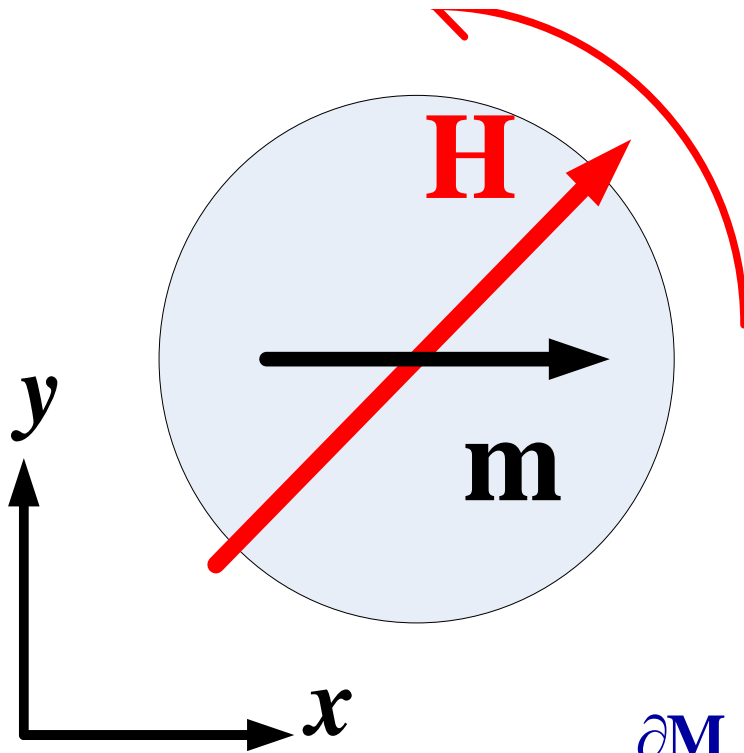
η = kinematic viscosity

- Viscous dominated regime
- Particle spin-velocity is no longer given by vorticity
- Magnetic torque density in Con of Ang Mom:

$$0 = \mu_0 \mathbf{M} \times \mathbf{H} + 2\zeta (\nabla \times \mathbf{v} - 2\boldsymbol{\omega})$$

Effect of Spin-velocity on Dynamics

Increasing frequency $\Omega > 1/\tau$

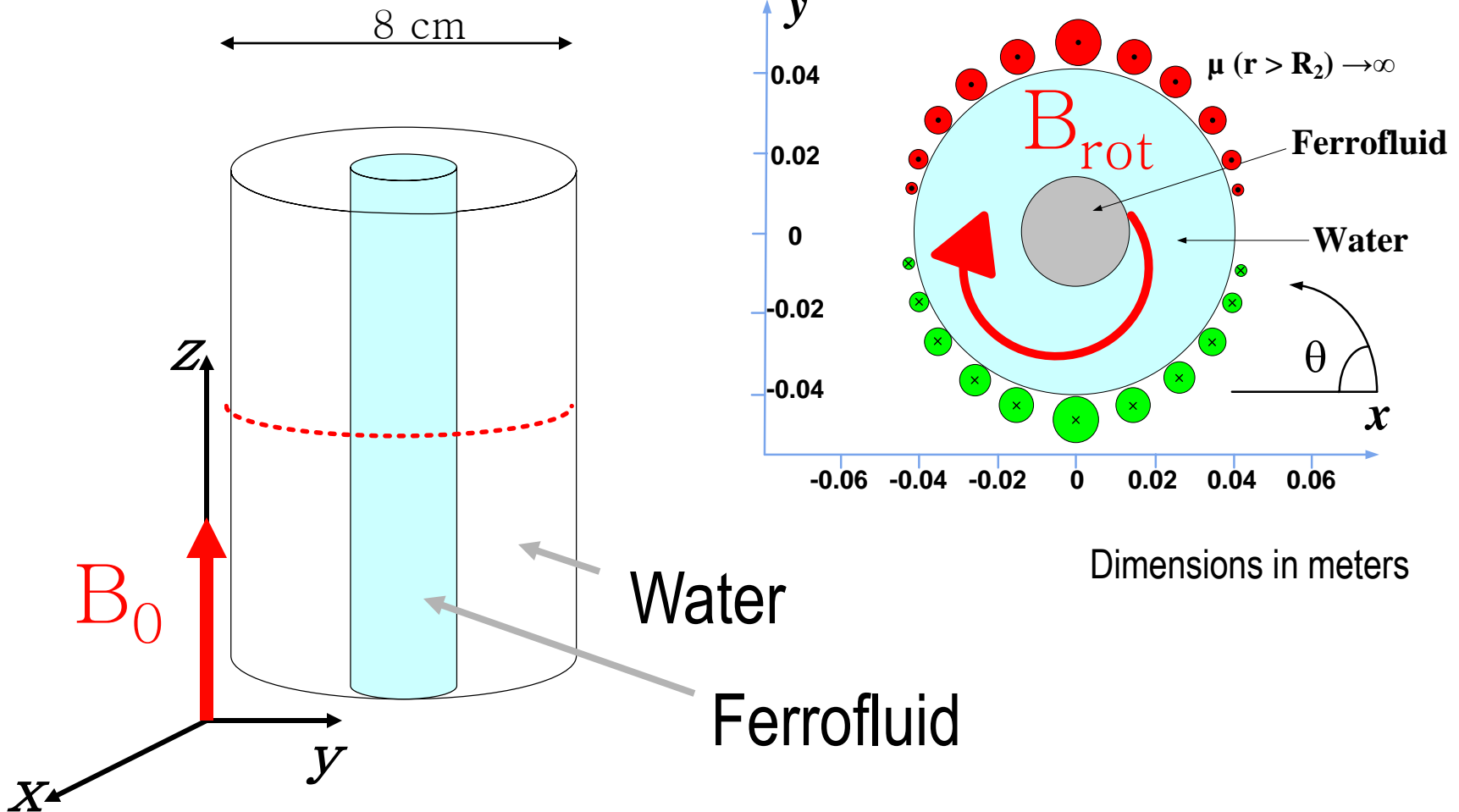


- \mathbf{M} and \mathbf{H} are related by a complex susceptibility
 - Ω (electrical frequency)
 - τ (ferrofluid time constant)
 - $\boldsymbol{\omega}$ (spin-velocity)
 - \boldsymbol{v} (flow velocity)

$$\frac{\partial \mathbf{M}}{\partial t} + (\boldsymbol{v} \cdot \nabla) \mathbf{M} - \boldsymbol{\omega} \times \mathbf{M} = -\frac{1}{\tau} (\mathbf{M} - \mathbf{M}_{eq})$$

Comsol Problem Definition

Concentric Cylinders of Water and Ferrofluid



Complex Susceptibility

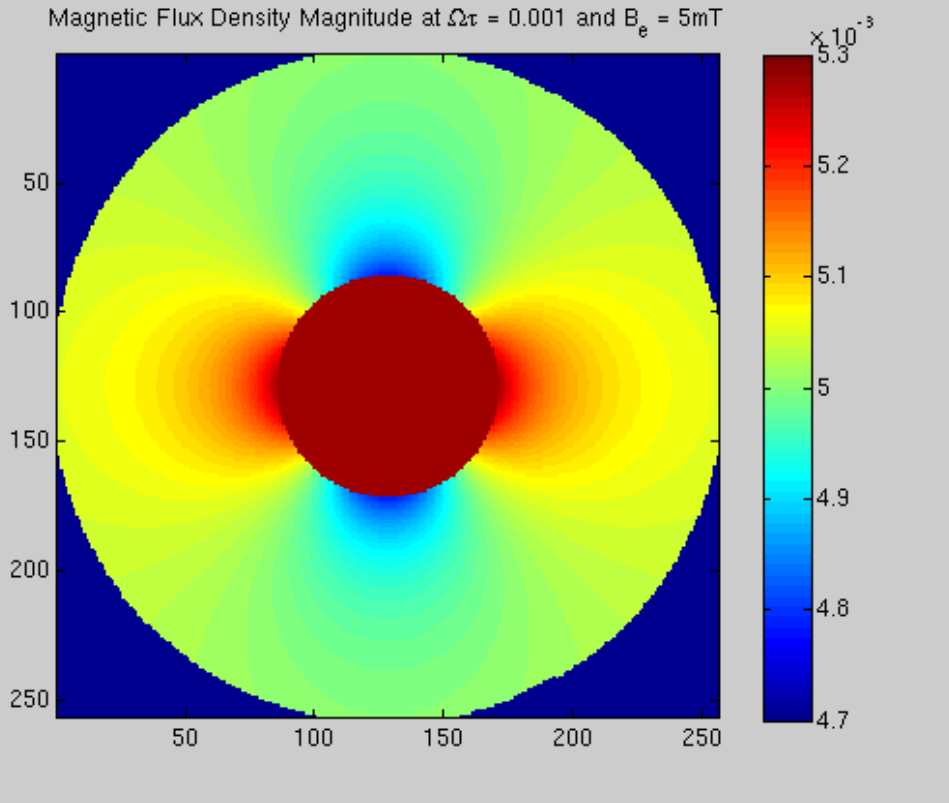
- Relating small-signal magnetic field to small-signal ferrofluid magnetization

$$\frac{\partial \mathbf{M}}{\partial t} + (\mathbf{v} \cdot \nabla) \mathbf{M} - \boldsymbol{\omega} \times \mathbf{M} = -\frac{1}{\tau} (\mathbf{M} - \mathbf{M}_{eq}) \xrightarrow{xy} \bar{\mathbf{m}} = \bar{\chi} \bar{\mathbf{h}}$$

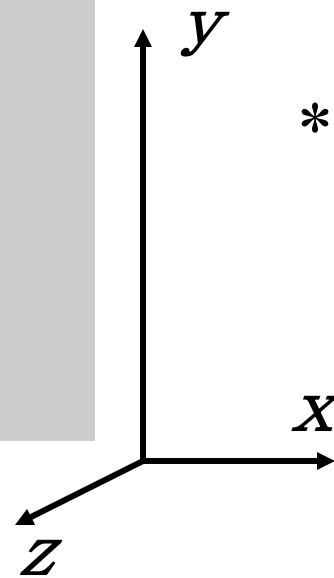
$$\begin{pmatrix} \mathbf{m}_x \\ \mathbf{m}_y \end{pmatrix} = \frac{M_0}{H_0} \frac{\begin{pmatrix} (1 + j\Omega\tau) & (\omega_z \tau) \\ -(\omega_z \tau) & (1 + j\Omega\tau) \end{pmatrix}}{(1 + j\Omega\tau)^2 + (\omega_z \tau)^2} \begin{pmatrix} \mathbf{h}_x \\ \mathbf{h}_y \end{pmatrix}$$

Exporting *Comsol* Results to *Matlab*

Instantaneous transverse B field



$$\Omega\tau = 0.001$$

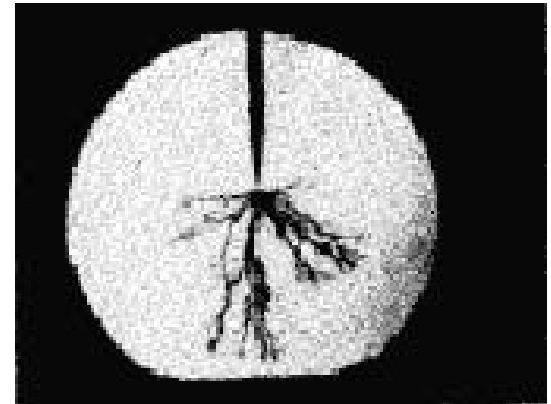


- * M and H are approx. collinear, H(t=0) is x-directed
- * Negligible spin-velocity

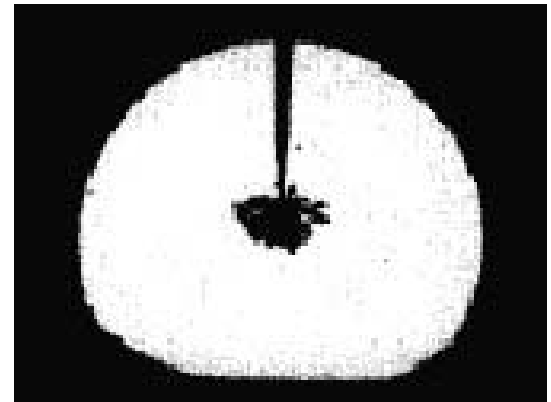
3. Applications to Increasing Power Transformer Electric Breakdown Strength

Electrical Streamer

- Streamers are low-density conductive structures that form when dielectric liquids are electrically over-stressed [2].
- Streamer characteristics are polarity dependent.
 - Positive Excitation: Filamentary structure, Breakdown velocities greater than 1 km/s, 4 propagation modes.
 - Negative Excitation: Bushy structure, Breakdown velocities greater than 100 m/s, 3 propagation modes.



Positive streamer growth in transformer oil. $V_{app} = 82$ kV, Gap $d = 1.27$ cm. [3]



Negative streamer growth in transformer oil. $V_{app} = 82$ kV, Gap $d = 1.27$ cm. [3]

Photos taken from:

J. C. Devins, *et al*, "Breakdown and Pre-breakdown Phenomena in Liquids," *J. Appl. Phys.*, 52 (7), July 1981.

Charge Generation Mechanisms

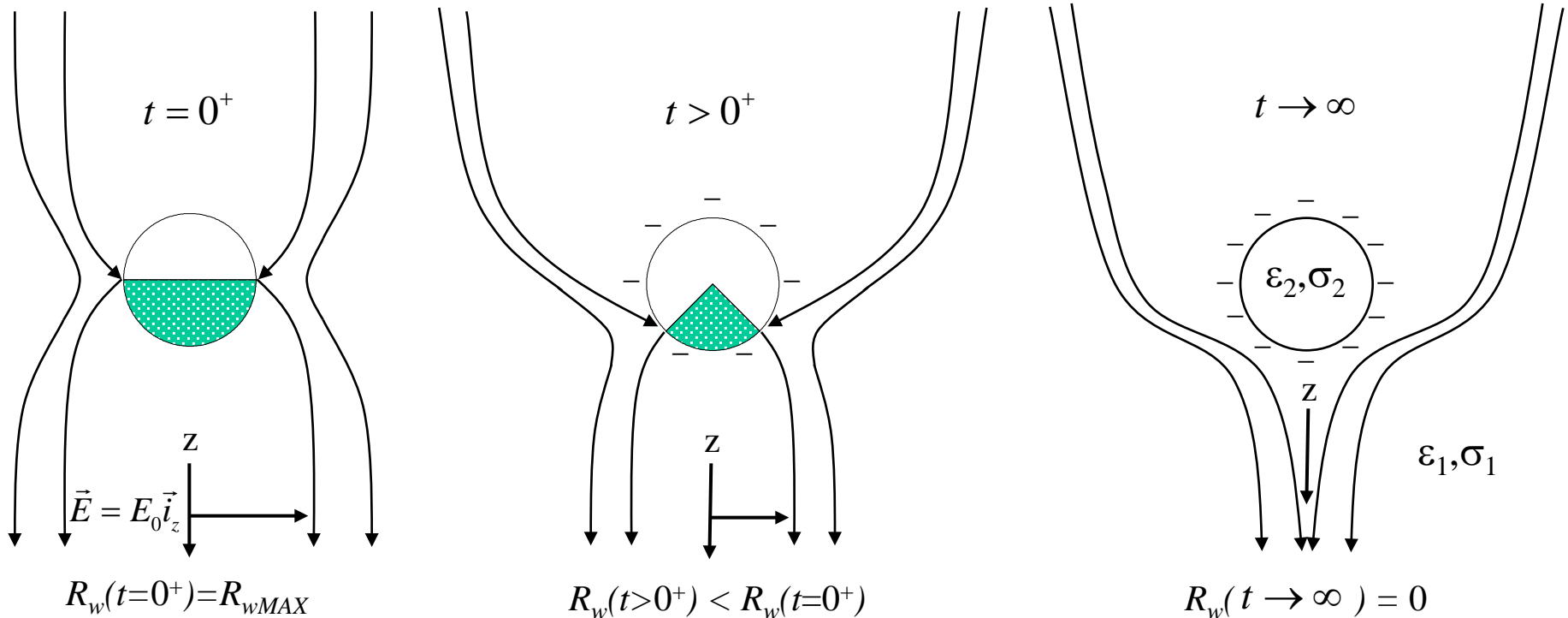
- ❑ Observable streamer structures are the result of electrically driven thermal dissipation.

- ❑ The role of four charge generation mechanisms have been explored.
 - Fowler-Nordheim electron injection (Unimportant)
 - Injection of electrons from a highly stressed negative electrode.
 - Electric field assisted ionic dissociation (Unimportant)
 - Generation of positive and negative ions due to dissociation of weakly bonded neutral ion-pairs at high electric fields.
 - Impact ionization (Unimportant)
 - Generation of positive ions and electrons due to inelastic collisions of free electrons that are accelerated in the high electric field levels.
 - Electric field dependent molecular ionization, Field ionization (Most Important)
 - Generation of positive ions and electrons due to the direct ionization of neutral molecules at high electric field levels.

Nanoparticle Charging Dynamics

- As a nanoparticle captures charge the electric field distribution in the vicinity of the particle changes with a decreasing charge capture window

$$Q(t) = \frac{Q_s}{1 + 4t/\tau}, \quad Q_s = 12\pi\epsilon E_0 R^2, \quad \tau = \frac{\epsilon}{\rho_0 \mu}$$



Electrodynamic Model for Nanofluid

- The trapping of electrons by nanoparticles in a nanofluid can be modeled by adding an attachment term to both the electron and negative ion continuity equations
- Heaviside function $H(\rho_{NPsat} - \rho_-)$ is used to account for the charge saturation of the nanoparticles
- Consider a 1 Gauss ferrofluid manufactured using 10 (nm) diameter particles:

$$n_0 = 3.4 \times 10^{20} \text{ (1/m}^3\text{)}$$

$$-\nabla \cdot (\epsilon \nabla V) = \rho_+ + \rho_- + \rho_e \quad \text{where} \quad \vec{E} = -\nabla V$$

$$\frac{\partial \rho_+}{\partial t} + \nabla \cdot \vec{J}_+ = G_I(|\vec{E}|) + \frac{\rho_+ \rho_e R_{+/e}}{e} + \frac{\rho_+ \rho_- R_{\pm}}{e}$$

$$\frac{\partial \rho_e}{\partial t} + \nabla \cdot \vec{J}_e = -G_I(|\vec{E}|) - \frac{\rho_+ \rho_e R_{+/e}}{e} - \frac{\rho_e}{\tau_a} - \frac{\rho_e}{\tau_{NP}} (1 - H(\rho_{NPsat} - \rho_-))$$

$$\frac{\partial \rho_-}{\partial t} + \nabla \cdot \vec{J}_- = \frac{\rho_e}{\tau_a} - \frac{\rho_+ \rho_- R_{\pm}}{e} + \frac{\rho_e}{\tau_{NP}} (1 - H(\rho_{NPsat} - \rho_-))$$

$$G_I(|\vec{E}|) = A_f |\vec{E}| \exp\left(-\frac{B_f}{|\vec{E}|}\right) \Rightarrow A_f = \frac{e^2 n_0 a}{h} \quad B_f = \frac{\pi^2 m^* a \Delta^2}{eh^2}$$

$$n_0 = 3.4 \times 10^{20} \text{ (1/m}^3\text{)}$$

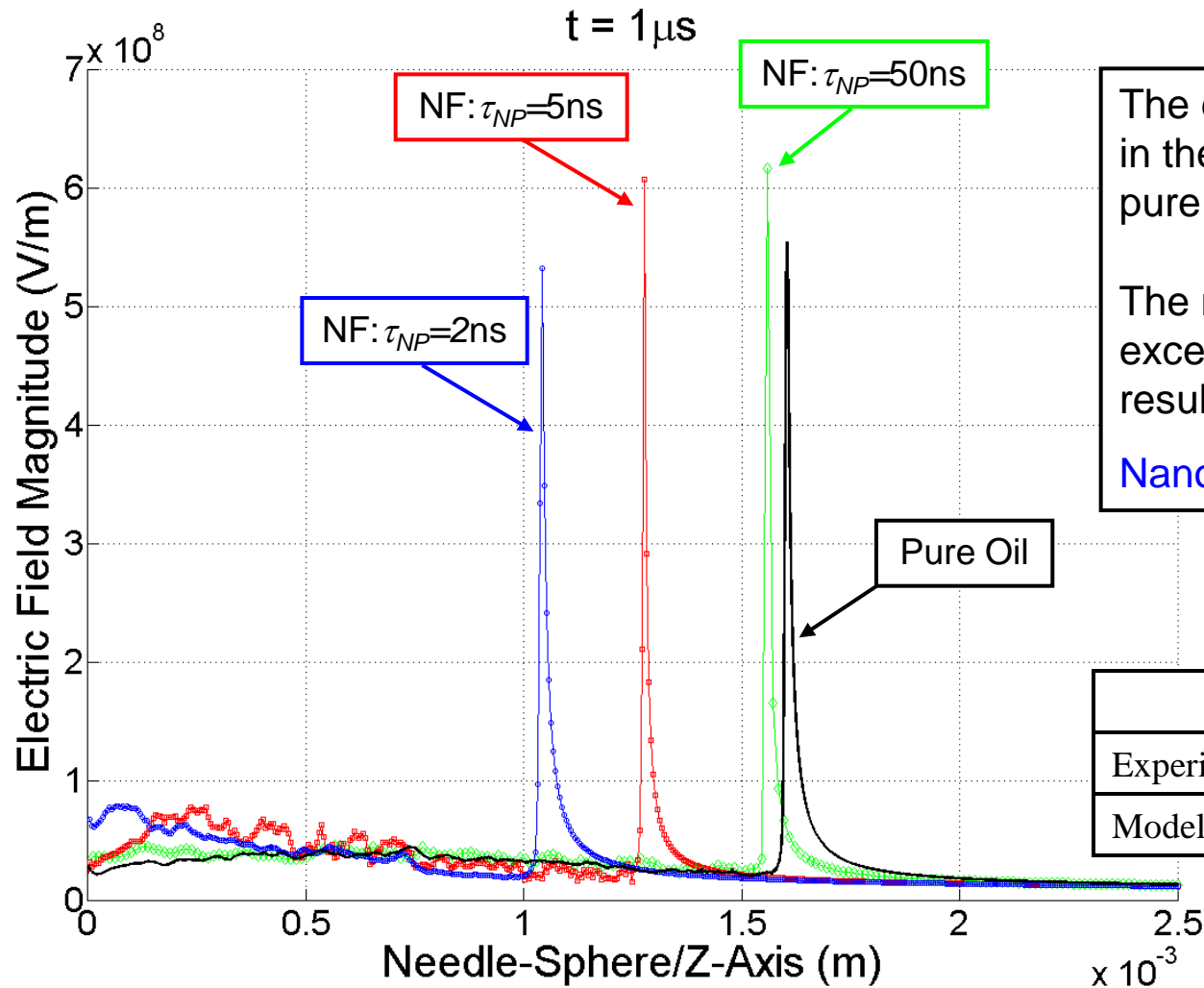
$$Q_S \approx -1.76 \times 10^{-18} \text{ (C)}$$

$$\approx 11 \text{ electrons}$$

$$\rho_{NPsat} = n_0 Q_S \approx -600 \text{ (C/m}^3\text{)}$$

Electric Field Dynamics in Nanofluids

- Simulations using nanoparticle attachment time constant values (τ_{NP}) of 2, 5 and 50 (ns)



The electric field wave propagation in the nanofluid is slower than in the pure oil

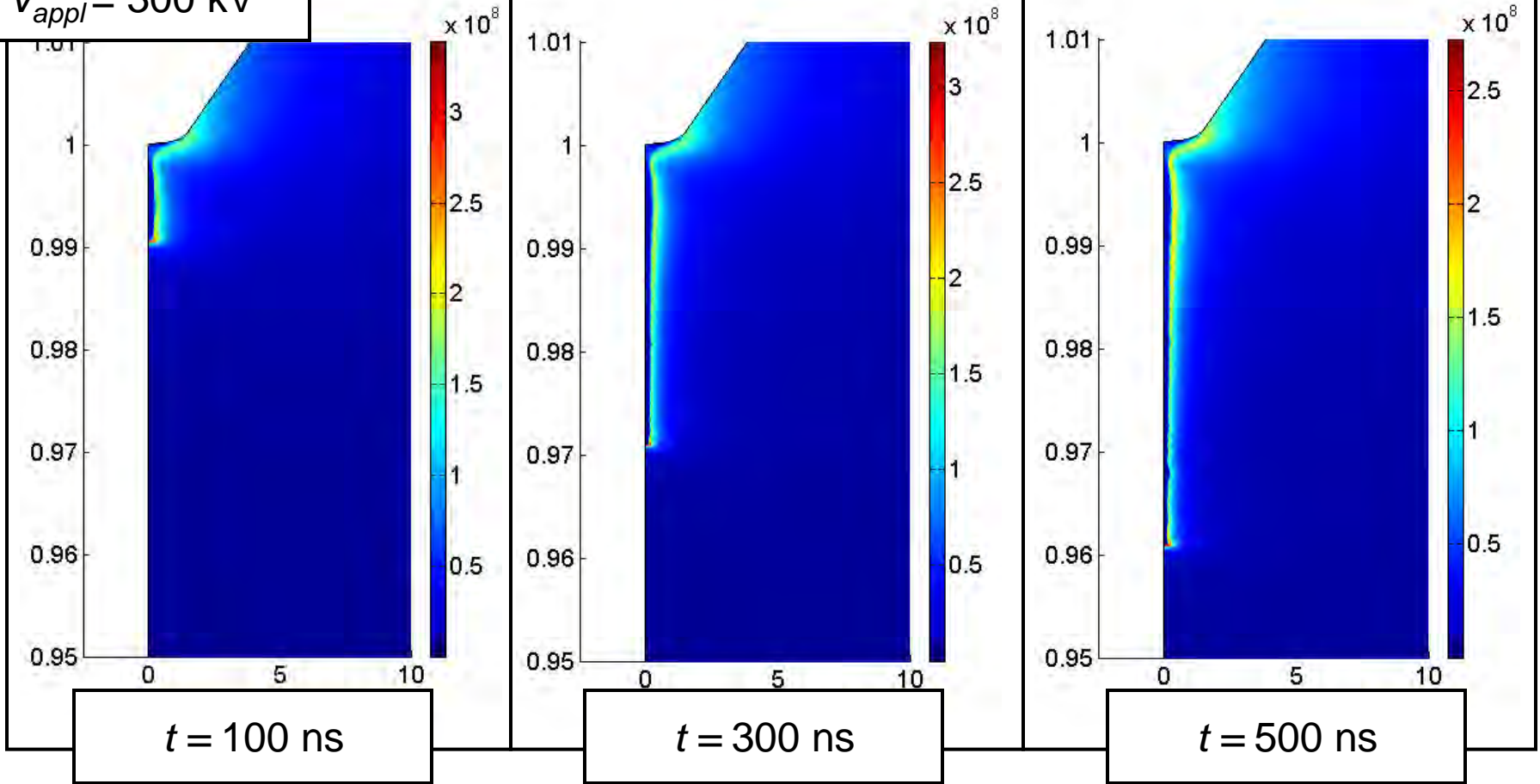
The model predictions correspond exceptionally well with experimental results

Nanoparticles must be conductive!!

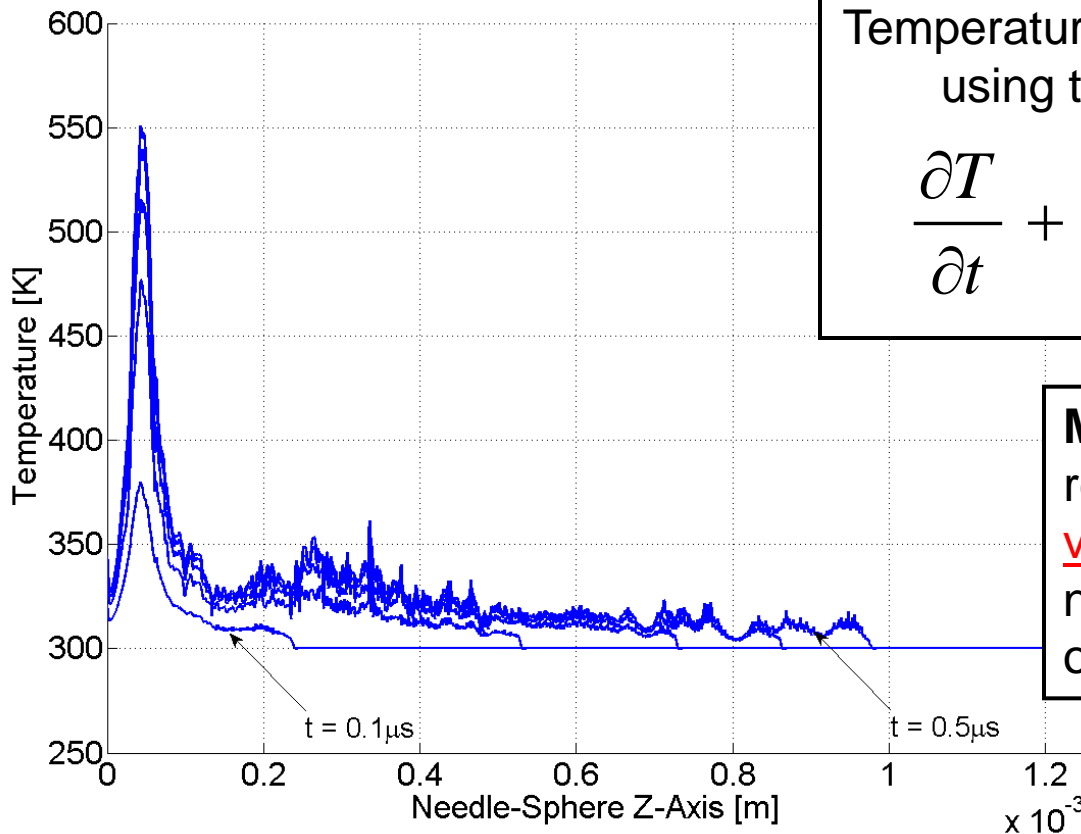
	Oil	NF
Experiment	1.59 km/s	1.02 km/s
Model	1.65 km/s	1.05 km/s

Results: Surface Electric Field

$V_{\text{appl}} = 300 \text{ kV}$



- Field ionization results in the development of a moving dissipative source that “sweeps” through the oil.

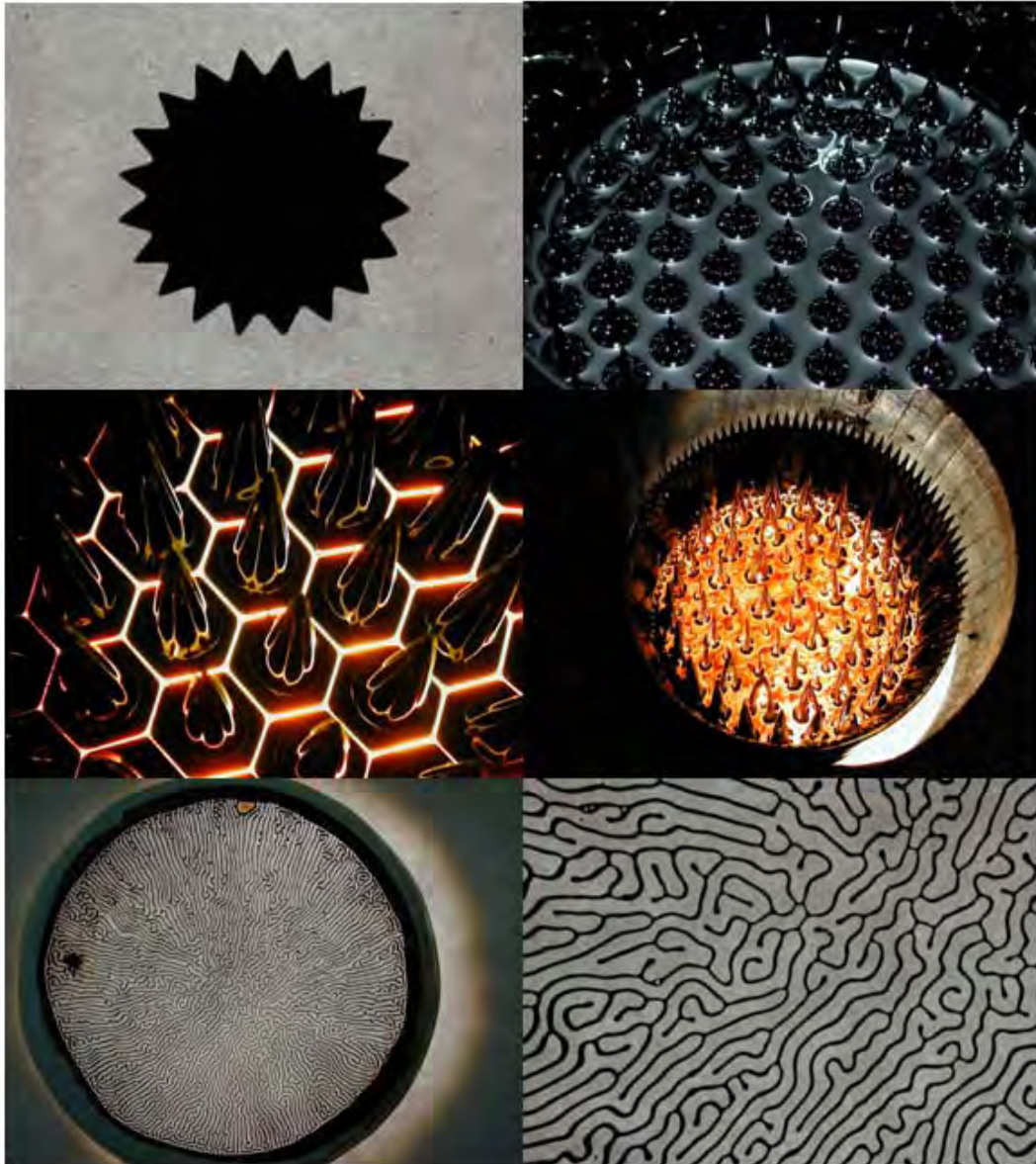


Temperature enhancement can be estimated using the thermal diffusion equation

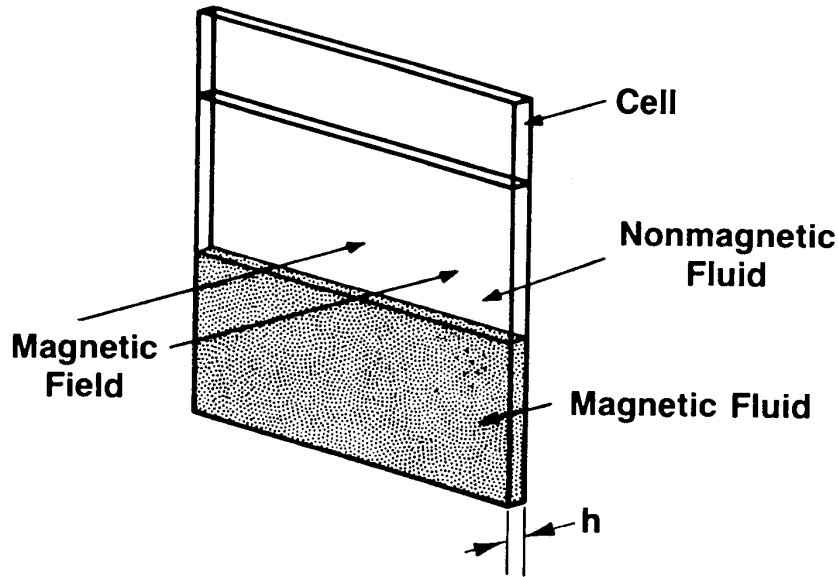
$$\frac{\partial T}{\partial t} + \vec{v} \cdot \nabla T = K_T \nabla^2 T + \frac{\vec{E} \cdot \vec{J}}{\rho_l c_v}$$

Major Result: Field ionization results in thermal enhancement values exceeding 200K which is needed overcome the latent heat of vaporization of transformer oil.

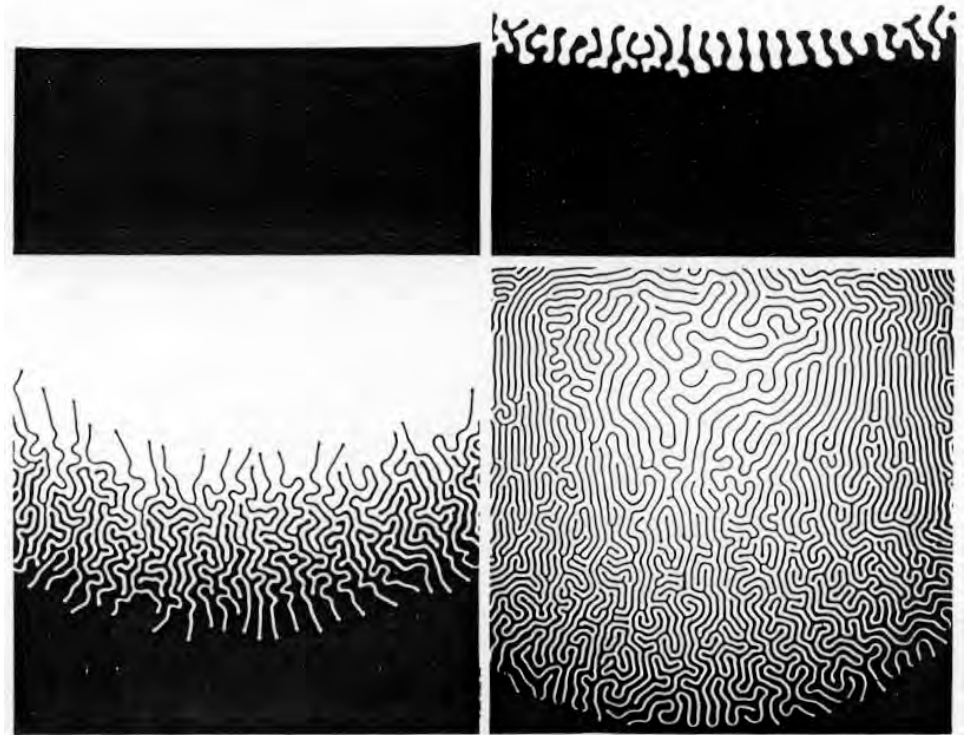
4. Ferrohydrodynamic Instabilities In DC Magnetic Fields



Labyrinthine Instability in Magnetic Fluids



Magnetic fluid in a thin layer with uniform magnetic field applied tangential to thin dimension.

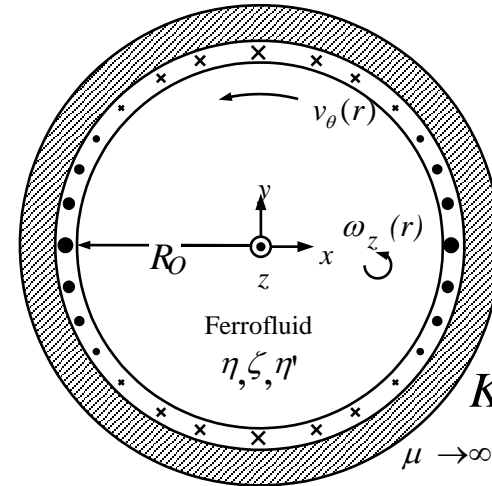
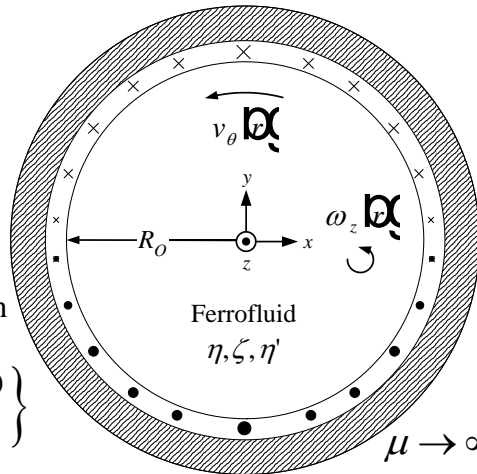


Stages in magnetic fluid labyrinthine patterns in a vertical cell, 75 mm on a side with 1 mm gap, with magnetic field ramped from zero to 535 Gauss.

Rotating Magnetic Fields

Uniform

Non-uniform

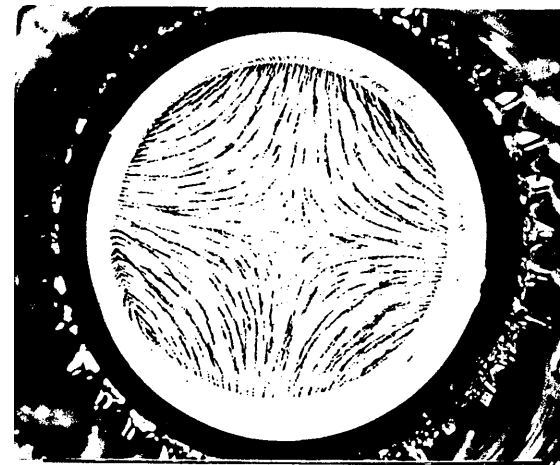
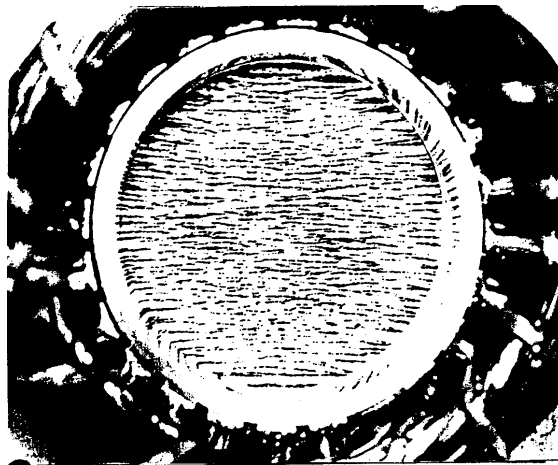


Surface Current Distribution

Surface Current Distribution

$$K_z = \text{Re} \left\{ K e^{j(\Omega_f t - \theta)} \right\}$$

$$K_z = \text{Re} \left\{ K e^{j(\Omega_f t - 2\theta)} \right\}$$



a. One pole pair stator

b. Two pole pair stator

Observed magnetic field distribution in the 3 phase AC stator

Ferrofluid Drops in Rotating Magnetic Fields



Traveling Wave
Pumping

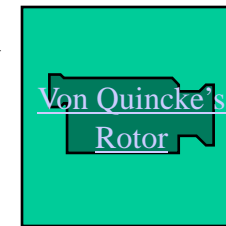
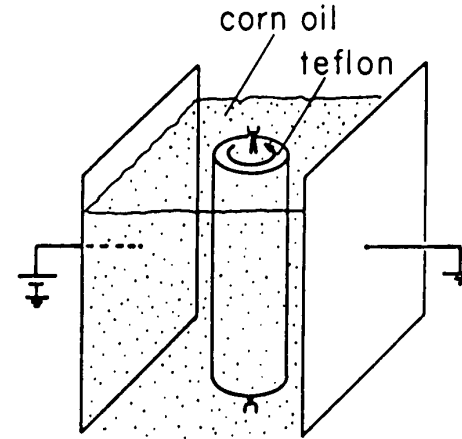
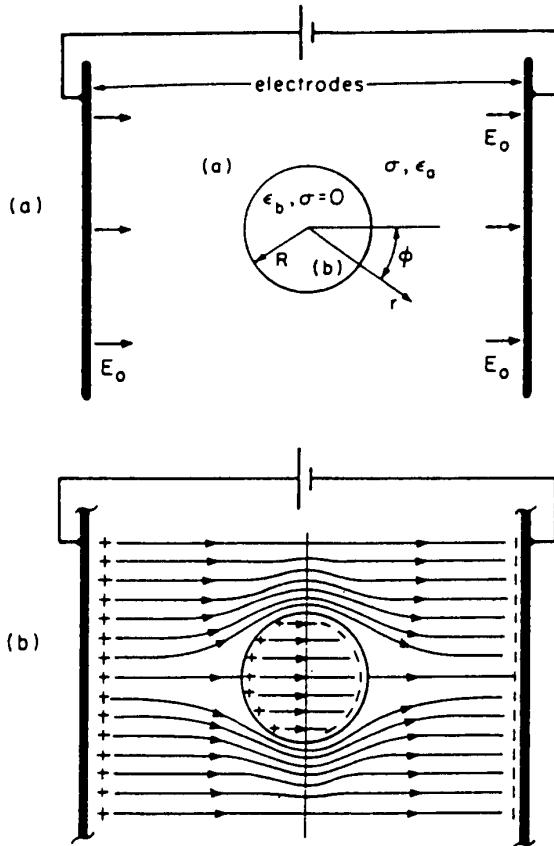
A Gallery of
Instabilities

Ferrohydrodynamic
Drops

Ferrofluid Spiral / Phase Transformations



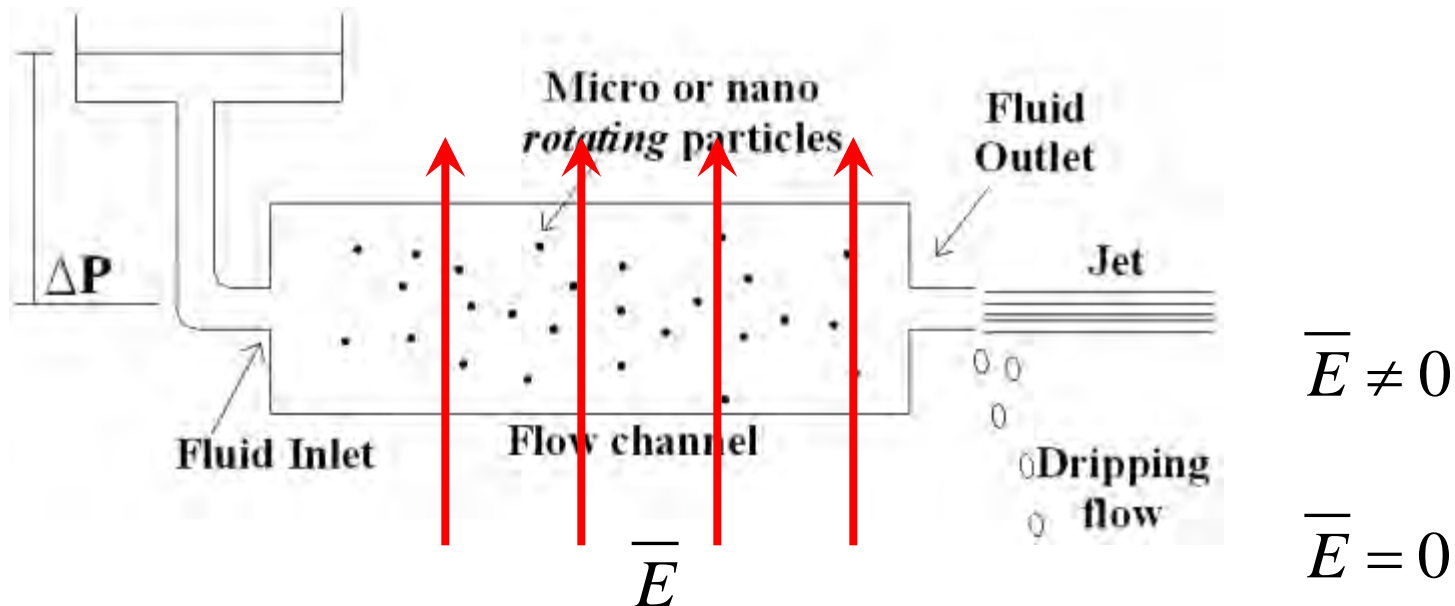
5. Dielectric Analog: Von Quincke's Rotor (Electrorotation)



(a) Von Quincke's rotor consists of a highly insulating cylinder that is free to rotate and that is placed in slightly conducting oil between parallel plate electrodes. As DC high voltage is raised, at a critical voltage the cylinder spontaneously rotates in either direction; (b) The motion occurs because the insulating rotor charges like a capacitor with positive surface charge near the positive electrode and negative surface charge near the negative electrode. Any slight rotation of the cylinder in either direction results in an electrical torque in the same direction as the initial displacement.

Electrorotation—Introduction

Experiments have shown that for a given pressure gradient, the Poiseuille flow rate can be increased (Lemaire et al., 2006) by introducing micro-particle electroration into the fluid flow via the application of an external direct current (DC) electric field.



Electrorotation—Quincke rotation

The electric torque $\overline{T}_e = \overline{p} \times \overline{E} = \frac{6\pi\varepsilon_1 R^3 E_0^2 (1 - \tau_1/\tau_2) \Omega \tau_{MW}}{(1 + 2\varepsilon_1/\varepsilon_2)(1 + \sigma_2/2\sigma_1)(1 + \Omega^2 \tau_{MW}^2)}$

For a small perturbation of rotation to grow, the torque balance on the particle is rewritten as (Jones, 1995):

$$I \frac{d\Omega}{dt} = \left[\frac{6\pi\varepsilon_1 R^3 E_0^2 (1 - \tau_1/\tau_2) \Omega \tau_{MW}}{(1 + 2\varepsilon_1/\varepsilon_2)(1 + \sigma_2/2\sigma_1)(1 + \Omega^2 \tau_{MW}^2)} - 8\pi\eta_1 R^3 \Omega \right]$$

The bracket term should have a value larger than zero for the small perturbation to grow (Jones, 1995), thus

$$\tau_2 > \tau_1$$

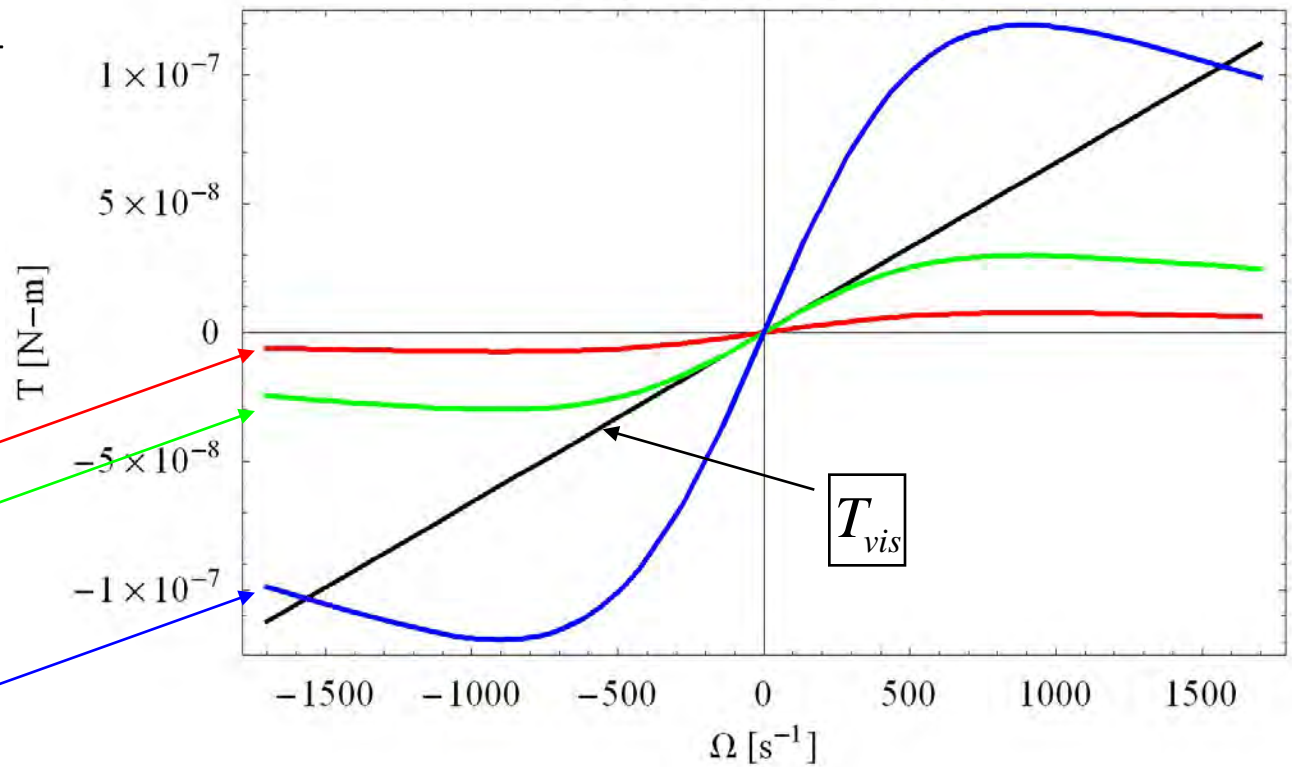
Electrorotation—Quincke rotation

$$E_{crit} = \left(1 + \frac{\sigma_2}{2\sigma_1}\right) \sqrt{\frac{8\eta_1\sigma_1}{3\varepsilon_1\sigma_2(\tau_2 - \tau_1)}}$$

$$E_0 > E_{crit}$$

Torque Solutions for Sphere

$$\Omega\tau_{MW} = \pm \sqrt{\left(\frac{E_0}{E_{crit}}\right)^2 - 1}$$



$T_e @ 0.5E_{crit}$

$T_e @ E_{crit}$

$T_e @ 2E_{crit}$

T_{vis}